

# Analytic Solution for the Drain Current of the Symmetric DG MOSFET

Adelmo Ortiz-Conde, Francisco J. García-Sánchez, Slavica Malobabic, and Juan Muci

Solid State Electronics Laboratory  
Simón Bolívar University, Caracas, Venezuela  
{ortizc, fgarcia, smalobabic}@ieee.org; jmuci@usb.ve

## ABSTRACT

A potential-based drain current model is presented for nanoscale undoped-body symmetric double gate MOSFETs. It is based on a fully coherent physical description and consists of a single analytic equation that includes both drift and diffusion contributions. The derivation is completely rigorous and based on a procedure previously enunciated for long-channel bulk SOI MOSFETs. The resulting expression is a continuous description valid for all bias conditions, from subthreshold to strong inversion and from linear to saturation operation. The validity of the model has been ascertained by extensive comparison to exact numerical simulations. The results attest to the excellent accuracy of this formulation.

**Keywords:** MOS compact modeling, Symmetric DG MOSFET, Undoped body MOS, Intrinsic channel, Drain current model.

## 1 INTRODUCTION

Double gate (DG) MOSFETs with undoped body (sometimes referred to as “intrinsic channel” MOSFETs) have become very attractive for scaling CMOS devices down to nanometer sizes [1]. These nanoscale devices permit the lessening of short-channel effects (SCEs) by means of an ultra thin body (UTB), instead of the usual high channel doping densities and gradients. The absence of dopant atoms in the channel reduces mobility degradation by eliminating impurity scattering and avoids random microscopic dopant fluctuations. Such advanced MOSFETs are being developed in several 3-D geometries [2, 3].

Highly accurate and physics based compact models which are at the same time computationally efficient are required for proper modeling of MOSFETs for VLSI circuit simulation. Explicit analytic models are highly desirable because they offer better computational efficiency than their numerical alternatives without loss of physical insight.

Taur [4, 5] obtained a system of two equations to describe the electrostatic potential across the silicon film. A charge-based drain current model (designated as Surface-Potential-Plus, SPP) was developed in 2004 by He [6] to avoid the numerical solution of the transcendental equation used in surface potential-based models. Recently a

continuous description was derived by Taur [7] for DG MOSFETs directly from Pao-Sah’s integral [8].

We have proposed an explicit approximate analytic solution of the surface potential of undoped-body symmetric DG devices [9], which was an extension of our previously proposed Lambert-W function-based analytic solution for the surface potential of undoped-body single-gate bulk devices [10]. Potential-based drain current models for the undoped-body symmetric DG MOSFET become more attractive with the advent of such analytic solutions.

In what follows we present the derivation of a physically consistent potential-based description of the drain current of undoped-body symmetric DG MOSFET. It is completely rigorous and is based on our previously proposed procedure to describe the current of long-channel bulk SOI MOSFETs [11]. The present result resembles the classical Pierret-Shields MOSFET model [12,13] more than Taur’s [7] because it contains the source and drain potentials explicitly.

This formulation should be understood as a core upon which complete compact models may be developed for these undoped-body symmetric DG devices. In that context, this drain current description does not intend to account for short-channel effects, carrier confinement energy quantization, interface roughness, ballistic-type transport, mobility degradation, etc.

## 2 DESCRIPTION OF THE POTENTIALS

In the undoped-body symmetric DG n-MOSFET, we define  $x$  as the direction across the channel thickness and  $y$  the direction along the channel. Here symmetric means that the two gates have the same work function, both gate oxides are of equal materials and thicknesses, and the same bias is applied to both gates.

It is assumed that the quasi-Fermi level is constant along the  $x$  direction, and current flows in the  $y$  direction. The energy levels are referenced to the electron quasi-Fermi level of the  $n^+$  source.

Considering that for an n-MOSFET the contribution of holes may be neglected and assuming potentials  $\psi \gg kT$ , the one-dimensional Poisson equation across the transverse direction  $x$  (body thickness) of this device, under the quasi-equilibrium approximation, leads to the following two equations [4, 5]:

$$V_{GF} = \psi_S + \frac{\sqrt{2kT n_i \epsilon_s}}{C_o} \sqrt{e^{-\beta V} \left( e^{\beta \psi_S} - e^{\beta \psi_o} \right)} \quad , \quad (1)$$

$$\psi_S = \psi_o - \frac{2}{\beta} \ln \left\{ \cos \left[ \sqrt{\frac{q^2 n_i}{2kT \epsilon_s}} e^{\frac{\beta(\psi_o - V)}{2}} \frac{t_{Si}}{2} \right] \right\} \quad , \quad (2)$$

where  $V_{GF}$  is the difference between the gate-to-source voltage and the flat-band voltage,  $\beta = q/kT$  is the inverse of the thermal voltage,  $n_i$  is the intrinsic carrier density,  $\psi_S$  is potential at the surface ( $x = t_{Si}/2$ ),  $\psi_o$  is the potential extremum at the center of the silicon film ( $x=0$ ),  $C_o$  is the gate oxide capacitance per unit area,  $\epsilon_s$  is the permittivity of the semiconductor,  $t_{Si}$  is the semiconductor film thickness,  $V$  is the difference between electron and hole quasi-Fermi levels along the channel (channel voltage), equal to 0 at the source and to  $V_{DS}$  at the drain.

Equations (1) and (2) must be solved to obtain the surface potential,  $\psi_S$ , and the center-of-film potential extremum,  $\psi_o$ , both at the source,  $y=0$ , and at the drain,  $y=L$ , ends of the channel. The solution at the source end, with  $V=0$ , gives:  $\psi_S = \psi_{S0}$  and  $\psi_o = \psi_{o0}$ . Analogously, solving at the drain end with  $V=V_{DS}$  produces:  $\psi_S = \psi_{SL}$  and  $\psi_o = \psi_{oL}$ .

### 3 DRAIN CURRENT FORMULATION

The drain current can be described following Pao and Sah's idea that including both the drift and diffusion carrier transport components in the silicon film results in a current description with smooth transitions between operating regions. Under the approximation that the mobility is independent of position in the channel, the current may be expressed as [12, 13]

$$I_D = \mu \frac{W}{L} \int_0^{V_{DS}} Q_I dV \quad , \quad (3)$$

where  $\mu$  is the effective electron mobility,  $W$  is the channel width,  $L$  is the effective channel length, and  $Q_I$  is the total (integrated in the transverse direction) inversion charge density inside the silicon film at a given location,  $y$ , along the channel defined by

$$Q_I \equiv -2q \int_0^{t_{Si}/2} (n - n_i) dx = -2q \int_{\psi_o}^{\psi_S} \frac{n - n_i}{F} d\psi \quad , \quad (4)$$

where  $F$  is the electric field.

Since  $n \gg n_i$  and there is no fixed charge in the undoped body,  $Q_I$  can be taken as being the total semiconductor charge:

$$Q_I = 2\epsilon_s F_s = -2C_o(V_{GF} - \psi_S) \quad . \quad (5)$$

where  $F_s$  is the electric field at the surface, and the "2" comes from the symmetry.

An equivalent to Pao-Sah's equation for the SOI MOSFET may be obtained by substituting (4) into (3)

$$I_D = 2\mu \frac{W}{L} \int_0^{V_{DS}} \int_{\psi_o}^{\psi_S} \frac{q n}{F} d\psi dV \quad , \quad (6)$$

with

$$n = n_i e^{\beta(\psi - V)} \quad , \quad (7)$$

and the electric field in the semiconductor film is given by

$$F = -\sqrt{\frac{2kT n_i}{\epsilon_s} e^{\beta(\psi - V)} + \alpha} \quad , \quad (8)$$

where

$$\alpha \equiv -\frac{2kT n_i}{\epsilon_s} e^{\beta(\psi_o - V)} \quad (9)$$

is defined as an interaction factor representing the charge coupling between the two gates, following our previous formulation [11].

We now proceed to evaluate the partial derivative of (8) with respect to channel voltage, following the procedure developed by Pierret and Shields [12, 13]:

$$\frac{\partial F}{\partial V} = \frac{1}{2F} \frac{d\alpha}{dV} - \frac{1}{F} \frac{q n_i}{\epsilon_s} e^{\beta(\psi - V)} \quad . \quad (10)$$

In the above equation we have written the total derivative  $d\alpha/dV$  because  $\alpha$  does not depend on  $\psi$ . Substituting (7) into (10) yields

$$\frac{q n}{F} = \epsilon_s \left( \frac{1}{2F} \frac{d\alpha}{dV} - \frac{\partial F}{\partial V} \right) \quad . \quad (11)$$

Further substitution of (11) into (6) gives

$$I_D = 2\mu \frac{W}{L} \epsilon_s \int_0^{V_{DS}} \int_{\psi_o}^{\psi_S} \left( \frac{1}{2F} \frac{d\alpha}{dV} - \frac{\partial F}{\partial V} \right) d\psi dV \quad . \quad (12)$$

### 4 EVALUATION OF THE INTEGRALS

Separating for convenience the two terms in the integrand of the double integral in (12) into two integrals,  $I_1$  and  $I_2$ , such that  $I = I_1 - I_2$ . The first integral may be integrated to yield

$$\begin{aligned}
I_1 &= \int_0^{V_{DS}} \int_{\psi_o}^{\psi_s} \frac{1}{2F} \frac{d\alpha}{dV} d\psi dV = \frac{1}{2} \int_0^{V_{DS}} \frac{d\alpha}{dV} \left( \int_{\psi_o}^{\psi_s} \frac{1}{F} d\psi \right) dV \\
&= \frac{1}{2} \int_0^{V_{DS}} \frac{d\alpha}{dV} \frac{t_{Si}}{2} dV = \frac{t_{Si}}{4} (\alpha_0 - \alpha_L)
\end{aligned} \tag{13}$$

where  $\alpha_0$  and  $\alpha_L$  represent the values of the coupling coefficient  $\alpha$  evaluated at the source and at drain ends, respectively. Next we proceed to calculate the integral  $I_2$ , defined by

$$I_2 = \int_0^{V_{DS}} \int_{\psi_o}^{\psi_s} \frac{\partial F}{\partial V} d\psi dV \tag{14}$$

Following Pierret and Shields' ideas [12] for the bulk device, we note that the region of integration falls between  $\psi_S$  and  $\psi_o$ , from  $V=0$  to  $V=V_{DS}$ . Integral  $I_2$  may be further broken up into four integrals:

$$\begin{aligned}
&\int_0^{V_{DS}} \int_{\psi_o}^{\psi_s} \frac{\partial F}{\partial V} d\psi dV = \\
&\int_0^{V_{DS}} \int_{\psi_m}^{\psi_{s0}} \frac{\partial F}{\partial V} d\psi dV + \int_0^{V_{DS}} \int_{\psi_{s0}}^{\psi_s} \frac{\partial F}{\partial V} d\psi dV, \tag{15} \\
&- \int_0^{V_{DS}} \int_{\psi_m}^{\psi_{o0}} \frac{\partial F}{\partial V} d\psi dV - \int_0^{V_{DS}} \int_{\psi_{o0}}^{\psi_o} \frac{\partial F}{\partial V} d\psi dV
\end{aligned}$$

where  $\psi_m$  is any value less than  $\psi_{o0}$  and its exact value is not important. Since the first and the third terms in the above equation have both constant limits of integration, the order of integration may be inverted, yielding

$$\begin{aligned}
\int_0^{V_{DS}} \int_{\psi_m}^{\psi_{s0}} \frac{\partial F}{\partial V} d\psi dV &= \int_{\psi_m}^{\psi_{s0}} \int_0^{V_{DS}} \frac{\partial F}{\partial V} dV d\psi \\
&= \int_{\psi_m}^{\psi_{s0}} [F(\psi, V = V_{DS}) - F(\psi, V = 0)] d\psi
\end{aligned} \tag{16}$$

and

$$\begin{aligned}
\int_0^{V_{DS}} \int_{\psi_m}^{\psi_{o0}} \frac{\partial F}{\partial V} d\psi dV &= \int_{\psi_m}^{\psi_{o0}} \int_0^{V_{DS}} \frac{\partial F}{\partial V} dV d\psi \\
&= \int_{\psi_m}^{\psi_{o0}} [F(\psi, V = V_{DS}) - F(\psi, V = 0)] d\psi
\end{aligned} \tag{17}$$

Changing the order of the integration in the second term of  $I_2$  in (15),

$$\int_0^{V_{DS}} \int_{\psi_{s0}}^{\psi_s} \frac{\partial F}{\partial V} d\psi dV = \int_{\psi_{s0}}^{\psi_{SL}} \int_{V_f}^{V_{DS}} \frac{\partial F}{\partial V} dV d\psi, \tag{18}$$

where  $V_f$  is the value of  $V$  at which the surface band bending is  $\psi_{sf}$ . Now integrating (18) produces

$$\begin{aligned}
&\int_0^{V_{DS}} \int_{\psi_{s0}}^{\psi_s} \frac{\partial F}{\partial V} d\psi dV = \\
&\int_{\psi_{s0}}^{\psi_{SL}} \left[ F(\psi, V = V_{DS}) - F(\psi, V = V_f) \right] d\psi
\end{aligned} \tag{19}$$

Also, the fourth term of  $I_2$  in (15) may be written as

$$\begin{aligned}
&\int_0^{V_{DS}} \int_{\psi_{o0}}^{\psi_o} \frac{\partial F}{\partial V} d\psi dV = \\
&\int_{\psi_{o0}}^{\psi_{oL}} [F(\psi, V = V_{DS}) - F(\psi, V = V_b)] d\psi
\end{aligned} \tag{20}$$

where  $V_b$  is the value of  $V$  at which the surface band bending is  $\psi_o$ . Substituting (16), (17), (19), and (20) into (15) and reordering yields

$$\begin{aligned}
&\int_0^{V_{DS}} \int_{\psi_o}^{\psi_s} \frac{\partial F}{\partial V} d\psi dV = \\
&\int_{\psi_{oL}}^{\psi_{SL}} F(\psi, V = V_{DS}) d\psi - \int_{\psi_{o0}}^{\psi_{s0}} F(\psi, V = 0) d\psi \\
&- \int_{\psi_{s0}}^{\psi_{SL}} F(\psi, V = V_f) d\psi - \int_{\psi_{o0}}^{\psi_{oL}} F(\psi, V = V_b) d\psi
\end{aligned} \tag{21}$$

Since  $\psi = \psi_{sf}$  for  $V = V_f$ , we recognize that  $F(\psi, V = V_f) = F_s$ . Therefore, the third term in (21) may be integrated using (5),

$$\begin{aligned}
&\int_{\psi_{s0}}^{\psi_{SL}} F(\psi, V = V_f) d\psi = \\
&\int_{\psi_{s0}}^{\psi_{SL}} F_s d\psi = \int_{\psi_{s0}}^{\psi_{SL}} \frac{C_o}{\epsilon_s} (V_{GF} - \psi_s) d\psi \\
&= \frac{C_o}{\epsilon_s} \left[ V_{GF} (\psi_{SL} - \psi_{s0}) - \frac{1}{2} (\psi_{SL}^2 - \psi_{s0}^2) \right]
\end{aligned} \tag{22}$$

Analogously, integrating the fourth term of (21) yields

$$\int_{\psi_{o0}}^{\psi_{oL}} F(\psi, V = V_b) d\psi = 0, \quad (23)$$

because the integrand is zero since it is the electric field at  $\psi = \psi_o$ . The integral in the second term of (21) may be evaluated using (8) and (9):

$$\begin{aligned} \int_{\psi_{o0}}^{\psi_{s0}} F(\psi, V = 0) d\psi &= - \int_{\psi_{o0}}^{\psi_{s0}} \sqrt{\frac{2kT n_i}{\epsilon_s} e^{\beta\psi} + \alpha_0} d\psi \\ &= \frac{2}{\beta} \sqrt{\frac{2kT n_i}{\epsilon_s}} \\ &\left[ \sqrt{e^{\beta\psi_{s0}} - e^{\beta\psi_{o0}} - e^{\frac{\beta\psi_{o0}}{2}}} \arctan\left(\sqrt{e^{\beta(\psi_{s0} - \psi_{o0})} - 1}\right) \right] \end{aligned} \quad (24)$$

Similarly, the integral in the first term of (21) is:

$$\begin{aligned} \int_{\psi_{oL}}^{\psi_{sL}} F(\psi, V = V_{DS}) d\psi &= - \int_{\psi_{oL}}^{\psi_{sL}} \sqrt{\frac{2kT n_i}{\epsilon_s} e^{\beta(\psi - V_{DS})} + \alpha_L} d\psi \\ &= \frac{2}{\beta} \sqrt{\frac{2kT n_i}{\epsilon_s}} e^{-\frac{\beta V_{DS}}{2}} \\ &\left[ \sqrt{e^{\beta\psi_{sL}} - e^{\beta\psi_{oL}} - e^{\frac{\beta\psi_{oL}}{2}}} \arctan\left(\sqrt{e^{\beta(\psi_{sL} - \psi_{oL})} - 1}\right) \right] \end{aligned} \quad (25)$$

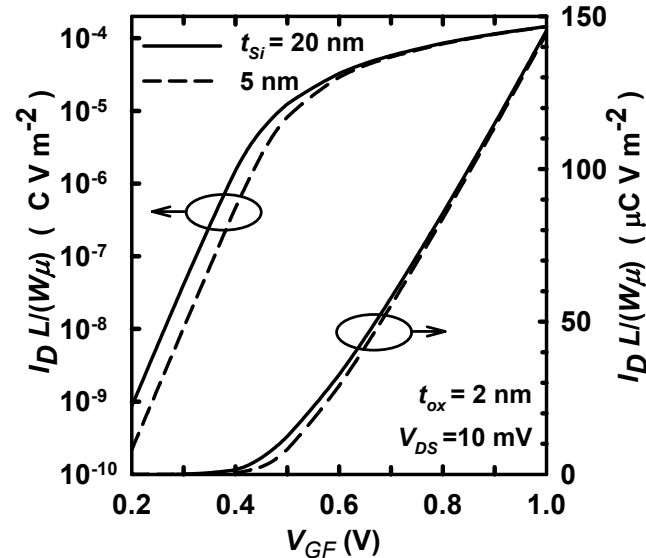


Fig. 1 Effect of semiconductor film thickness on drain current at low drain voltage.

Some algebraic and trigonometric manipulations of (2), (5), (8), (9), (12), (13), (15), (17), (21)-(25), yield the following general current-voltage equation valid for all bias conditions [14]:

$$\begin{aligned} I_D = \mu \frac{W}{L} \left\{ 2C_o \left[ V_{GF}(\psi_{sL} - \psi_{s0}) - \frac{1}{2}(\psi_{sL}^2 - \psi_{s0}^2) \right] \right. \\ \left. + 4 \frac{kT}{q} C_o (\psi_{sL} - \psi_{s0}) \right. \\ \left. + t_{Si} kT n_i \left[ e^{\beta(\psi_{oL} - V_{DS})} - e^{\beta\psi_{o0}} \right] \right\} \end{aligned} \quad (26)$$

Figures 1 and 2 present the current, divided by  $\mu W/L$ , as a function of gate voltage for different values of  $t_{ox}$  and  $t_{Si}$ , as calculated by the present analytic description.

It is important to point out that equation (26) is equivalent to equation (6) in [7], although the derivation was different.

This equivalence can be established, after some algebraic manipulations, by noting that the beta parameter,  $\beta_T$ , introduced in [7] is related to the charge coupling factor  $\alpha$  between the two gates, defined in (9) and originally proposed by us [11], by the following relation:

$$\beta_T \equiv -\alpha \left/ \left( 4 \frac{kT}{q t_{Si}} \right)^2 \right. \quad (27)$$

Other approximate charge-based expressions for the current that have been proposed [6,15] may be related to the present formulation or to Taur's expression [7].

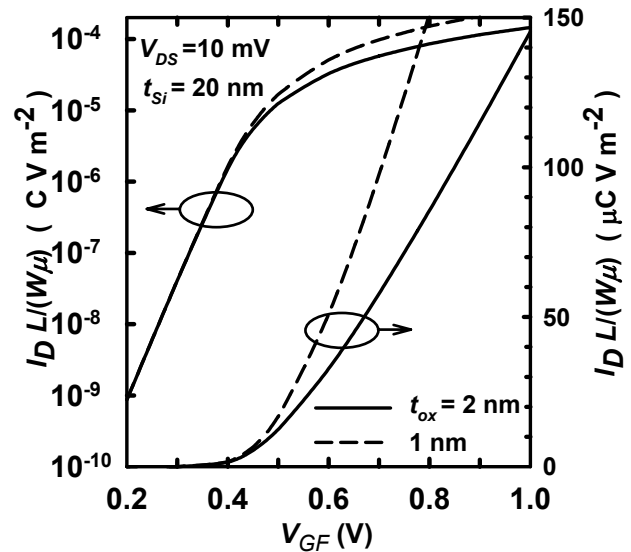


Fig. 2 Effect of gate oxide thickness on drain current at low drain voltage.

## 5 COMPARISON TO EXACT NUMERICAL SIMULATIONS

The drain current in (26) is essentially exact within the bounds of its formulation and should produce the same results as direct numerical integration of the carrier charge along the channel indicated by (3). Figure 3 shows the drain current as a function of drain voltage, calculated by the present analytic description using (26), and exact results from numerical integration of the charge along the channel with increments of 1mV. The surface and center-of-film potentials needed in (26), and the carrier charge, used for the direct numerical integration, were calculated by iteratively solving (1) (2). The current is presented for convenience divided by  $\mu W/L$ , with the channel dimensions assumed to be much larger than its thickness.

Comparison of the two results demonstrates the excellent accuracy of the present analytic description of the current. The resulting errors fall well below  $10^{-17}$  for all operating regions, as shown in the plots at the bottom of Fig. 3. Considering that 20 digit precision was used in the numerical calculations, this represents a negligible error within computational accuracy.

It should be noted that the surface and center-of-film potentials may be obtained using an approximate analytical solution [9], as already mentioned in the introduction.

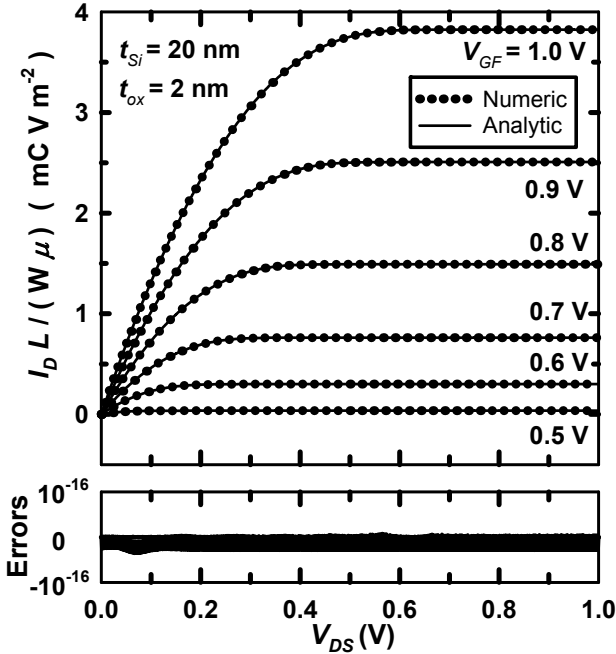


Fig. 3 Drain current as a function of drain voltage for several values of gate voltage. Calculated using (26): solid lines. Direct numerical integration: symbols.

## 6 ANALYSIS OF THE COMPONENTS

In weak inversion, the first term in (26) is negligible. The third term is negative, but together with the second term gives a positive value approximated by:

$$I_{Dw} \approx \mu \frac{W}{L} t_{Si} k T n_i \left[ e^{\beta \psi_{o0}} - e^{\beta(\psi_{oL} - V_{DS})} \right]. \quad (28)$$

The observed vertical displacement of the curves in Fig. 1 corresponding to two film thickness is what is expected below threshold from the presence of  $t_{Si}$  in (28).

The strong inversion term can be obtained by subtracting the weak component from the total current:

$$I_{Ds} = I_D - I_{Dw}. \quad (29)$$

Figure 4 presents normalized  $I_D$ ,  $I_{Dw}$  and  $I_{Ds}$ , separately plotted versus gate voltage in order to analyze their relative importance. We observe that the total current is approximated by  $I_{Ds}$  above threshold and by  $I_{Dw}$  below threshold.

## 7 THRESHOLD

According to the analysis of the preceding section, the intersection of the two current components shown in Fig. 4 may be understood as the transition threshold from weak to strong inversion.

Figure 5 shows this intersection numerically calculated as a function of gate oxide,  $t_{ox}$ , with silicon film thicknesses,  $t_{Si}$ , as parameter. As it can be seen, the position of the intersection on the gate voltage axis, or apparent threshold voltage, decreases as  $t_{ox}$  and  $t_{Si}$  increase. The reduction of threshold with increasing  $t_{ox}$ , which is typical of undoped body devices, is opposite to that of conventional highly doped body MOSFETs. This behavior was first predicted analytically by us for the case of the undoped body MOS capacitor [10] and recently confirmed by 2-D simulations [16].

In order to obtain this intersection analytically, we approximate the weak and the strong inversion currents for small  $V_D$ . Below threshold the potential is essentially flat across the silicon film thickness because the drift current is negligible. Therefore,  $\psi_{SL} \approx \psi_{S0} \approx \psi_{oL} \approx \psi_{o0} \approx V_{GF}$ , and:

$$I_{Dw} = \mu \frac{W}{L} t_{Si} q n_i e^{\beta V_{GF}} V_{DS}, \quad (30)$$

and above threshold:

$$I_{Ds} = \mu \frac{W}{L} Q_{bulk} V_{DS}, \quad (31)$$

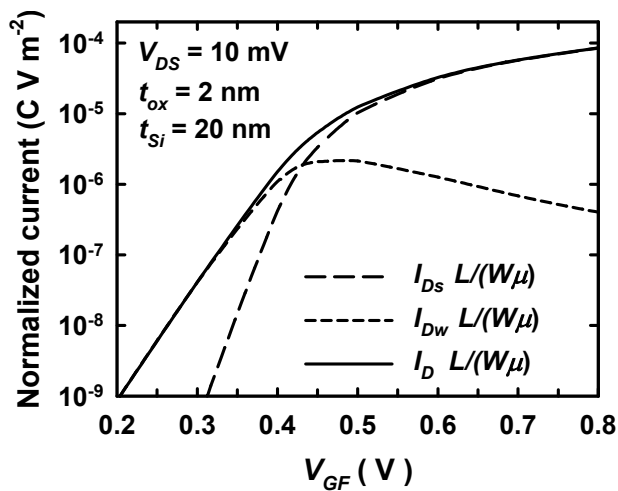


Fig. 4 Drain current as defined in (26) and its two components  $I_{Dw}$  and  $I_{Ds}$ .

where

$$Q_{bulk} = \frac{4 C_o}{\beta} W \left( \frac{q\sqrt{2}}{2 C_o} \sqrt{\frac{\epsilon_s n_i}{kT}} e^{\frac{\beta V_{GF}}{2}} \right) \quad (32)$$

is the charge for an undoped bulk MOSFET, where  $W$  is the Lambert function [10]. Finally, equating (30) and (31) gives the approximate location of their intersection on the gate voltage axis:

$$V_{Tx} = \frac{kT}{q} \left[ \ln \left( \frac{8 kT \epsilon_s}{q^2 n_i t_{Si}^2} \right) - W \left( \frac{4 \epsilon_s}{C_o t_{Si}} \right) \right]. \quad (33)$$

This approximate value from (33) decreases with both increasing  $t_{ox}$  and increasing  $t_{Si}$ . It is also shown in Fig. 5 to compare it to the numerically calculated intersection of (28) and (29).

## 8 CONCLUSIONS

A derivation of nanoscale undoped-body symmetric double gate MOSFETs drain current has been presented. It is physical and fully consistent in the classical sense. It follows a Pierret and Shields' type formulation considering diffusion and drift transport. The description is in terms of surface and center-of-film potentials evaluated at the source and drain ends of the channel.

The resulting expression is a single explicit analytic equation continuously valid for all bias conditions, from subthreshold to strong inversion and from linear to saturation operation, which makes it ideally suited as a core for full compact models. The negligible errors observed in extensive comparisons to exact numerical simulations demonstrate its excellent accuracy.

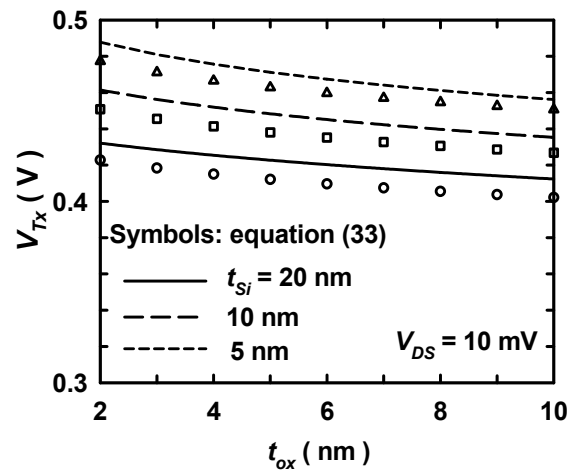


Fig. 5 Intersection of the two current components. From (28) and (29): lines. From (33): symbols.

## REFERENCES

- [1] Q. Chen, K.A. Bowman, E.M. Harrell, J.D. Meindl, IEEE Circuits and Devices Magazine, 19, 28-34, 2003.
- [2] J.P. Colinge, Solid-St. Electron. 48, 897-905, 2004.
- [3] D. Jiménez, B. Íñiguez, J. Suñé, L.F. Marsal, J. Pallarés, J. Roig, D. Flores, IEEE Electron Device Lett, 25, 571-573, 2004.
- [4] Y. Taur, IEEE Electron Device Lett, 21, 245-247, 2000.
- [5] Y. Taur, IEEE Trans on Electron Devices, 48, 2861-2869, 2001.
- [6] J. He, X. Xi, C.H. Lin, M. Chan, A. Niknejad, C. Hu. Workshop on Compact Modeling, NSTI-Nanotech, Boston, Massachusetts, 2, 124-127, 2004.
- [7] Y. Taur, X. Liang, W. Wang, H. Lu, IEEE Electron Device Lett, 25, 107-109, 2004.
- [8] H.C. Pao, C.T. Sah, Solid-St. Electron. 9, 927-937, 1966.
- [9] S. Malobabic, A. Ortiz-Conde, F.J. García Sánchez, Proc. 5th. IEEE Int. Conf. on Dev. Circ. and Syst, ICCDCS, Punta Cana, Dominican Republic, 19-25, 2004.
- [10] A. Ortiz-Conde, F.J. García Sánchez, M. Guzmán, Solid-St. Electron. 47, 2667-2674, 2003.
- [11] A. Ortiz-Conde, R. Herrera, P.E. Schmidt, F.J. García Sánchez, J. Andrian, Solid-St. Electron. 35, 1291-1298, 1992;.
- [12] R.F. Pierret, J.A. Shields, Solid-St. Electron. 26, 143-147, 1983.
- [13] J.J. Liou, A. Ortiz-Conde, F.J. García Sánchez, "Design and Analysis of MOSFETs: Modeling, simulation and parameter extraction," Kluwer Academic Publishers 1998.
- [14] A. Ortiz-Conde, F.J. García Sanchez, J. Muci, "Rigorous analytic solution for the drain current of undoped asymmetric dual-gate MOSFETs," Solid-State Electronics, in press, 2005.
- [15] J.M. Sallese, F. Krummenacher, F. Pregaldiny, C. Lallement, A. Roy, C. Enz, Solid-St. Electron. 49, 485-489, 2005.
- [16] M. Wong, X. Shi, IEEE Trans on Electron Devices, 51, 1600-1604, 2004.